Production and Properties of High-Serviceability Rail

H. MASUMOTO, K. SUGINO, S. NISHIDA, M. HATTORI, AND T. TERADA

In order to improve the serviceability of rails, the service life of a rail was divided into several elementary processes and the requisites for every process were investigated. The results of this study proved that increasing the strength of rails through pearlite refining, austenite grain refining, and preservation of compressive residual stress was effective in improving rail serviceability. High strength and a fine pearlitic microstructure increase the wear resistance of rails and deter the initiation of contact fatigue cracking on the surface of rails. Compressive residual stress delays fatigue crack propagation. One type of rail that satisfies these requirements is head-hardened rail. The head of these rails is slack quenched by blown air after austenitizing to cause the isothermal pearlite transformation. The hardened zone of this rail has a yield stress and tensile strength that exceed 800 MPa and 1200 MPa, respectively, and very fine pearlitic microstructure. This head-hardened rail also has a compressive residual stress of about 400 MPa on the running surface and on the sides of rail head. It has also been confirmed that this rail performs well in heavy-load railways.

Improving the serviceability of a rail will mean extending the service life of a rail. The service life begins at the time when the wheel contacts the rail for the first time, and the service life ends when the rail cannot bear the requisite load any longer due to a reduction of the rail-head area or when a fatigue crack grows severe enough to cause brittle fracture.

A rail of high serviceability must perform well throughout its service life, but it is very difficult to investigate the requisites for this type of rail simultaneously. If the service life of a rail is divided into several elementary deteriorating processes, the rail characteristics necessary for withstanding each process can be clarified and these characteristics can be incorporated in a single rail. Thus, it should be possible to develop a rail of high serviceability. This paper investigates these requisites and describes the properties of rails.

INVESTIGATIONS INTO REQUISITES FOR HIGH SERVICEABILITY

The service life of a rail can be divided into the elementary processes shown in Figure 1. Although the rate of each deterioration process is not necessarily clear, the deformation of the rail head and fatigue-crack propagation obviously must figure decisively in the determination of service life. The rail characteristics necessary for delaying these two processes were mainly investigated in laboratory and track tests.

First, increasing strength (especially yield strength) is indispensable for the prevention of plastic deformation on metal flow of the rail head. Increasing strength, together with increasing the rail section, has been an effective means of helping rails withstand increasing axle load and train speed and will continue to be a fundamental measure for prolonging rail service life in the future. At present, high-strength rails are classified into two groups: (a) one is as-rolled alloy-steel rails, which contain such alloying elements as Si, Mn, Cr, Mo, V, and Nb, and (b) the other heat-treated (either by full- or head-hardening) carbon-steel rails. According to the production methods employed, the microstructure of the rails changes into fine pearlite, tempered martensite, and bainite. These rails are shown in Figure 2. In this paper, investigations were made on high-strength rails with tensile strength more than 1100 MPa. In view of the increase in the superficial hardness of the rail head in service, the increase in strength through plastic deformation or work hardening should not be ignored.

It is said that the wear resistance of a rail can be improved by increasing its strength; therefore, a Nishihara-type wear test (1) was performed on specimens cut from high-strength rails of representative microstructures. Figure 3 shows the Nishihara-type wear-test method. In Figure 4 the weight loss of the specimen after 500 000 rotations is plotted against the hardness before the test. This weight loss correlates well with the amount of rail-head wear in the actual track. Figure 4 clearly indicates that weight loss decreases when hardness is increased and, at the same time, if the hardness is constant, pearlite shows the least weight loss among the three types of microstructure. One of the reasons why pearlite shows the least wear is its high work hardenability and its large volume of iron carbide. In Figure 5, weight loss of another test specimen is plotted against the superficial hardness of the specimen after the wear test. The weight loss is nearly determined by this superficial hardness, and the Vickers hardness increase through the wear test is about 150 and 240-300 for tempered martensite and pearlite, respectively, irrespective of initial hardness. These results indicate that the increase in strength through pearlite refining is very effective in improving wear resistance and that the morphology of cementite provides a valuable clue to the wear mechanism.

The initiation of defects on the rail surface in contact with train wheels is a problem of lubricated rail of less wear on railways with rather light axle loads. But the initiation of surface defects was also investigated on rails of the same kind of wear test by a rolling-contact fatigue test (1,2). Figure 6 shows the rolling-contact fatigue-test method,

Figure 1. Elementary processes of service life of rail.

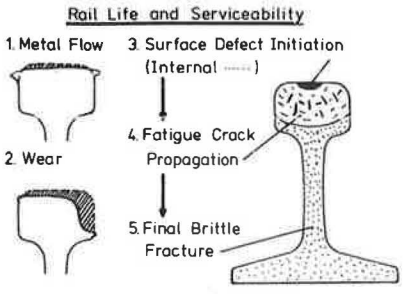

Figure 2. High-strength rails in Japan classified by production method and microstructure.

As-rolled	Alloy Steel	Low Carbon (C<0.4%)	Bainite	×
		Medium C (0.4-0.6%)	(Fine) Pearlite	⊘
		High C (0.6%<C)		●
Head Hardened	Slack Quenched	Carbon Steel,	Fine Pearlite	■
	Quenched & Tempered	Low Alloy Steel	Tempered Martensite	▲

Note: The symbols in this figure coincide with those in Figures 4, 5, and 7.

which is a modification of the Nishihara-type wear-test method. The number of specimen rotations before the first surface crack is detected on the specimen is processed according to the Weibull probability distribution; the results are shown in Figure 7. The longest service life up until the first crack initiation was obtained by high-strength rail of very fine pearlitic microstructure. Therefore, fine pearlite proved to be effective in preventing surface-defect initiation due to contact fatigue.

Besides surface-crack initiation, the internal initiation of fatigue cracking can also be a problem. These cracks generally initiate from large nonmetallic inclusions and cause transverse fractures (3,4). When the strength of a rail is increased, the steel becomes more sensitive to crack initiation from inclusions. Therefore, measures should be adopted to reduce the numbers of inclusions and control the shape of inclusions.

By the application of a cyclic load, the crack starts its growth as a fatigue crack. Next, the fatigue-crack propagation rate was investigated for the sample plates and high-strength rails (5). Specimen preparation is shown in Figure 8. At first, the crack-propagation rate was measured on the plates whose strength and austenite grain size were changed by heat treatment. Details about these sample plates are shown in Table 1, and the chemical composition of the pearlite-steel samples is given in the table below (in percent):

Sample Steel	C	Si	Mn	P	S	Cr
Carbon	0.68	0.22	0.87	0.017	0.016	-
1 percent Cr	0.75	0.30	0.30	0.018	0.020	1.00

[In Tables 1, 3, and 5 and in Figure 15, the following abbreviations are used: grain size number (GSN), proof stress (PS), tensile strength (TS), elongation (El), reduction of area (RA), and Vickers hardness number (VHN).] The sample plate microstructure is pearlite except sample G, which is tem-

Figure 3. Nishihara-type wear-test method.

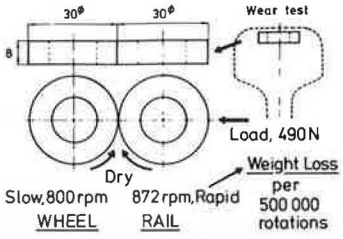

Figure 4. Effect of hardness and microstructure on weight loss by wear test.

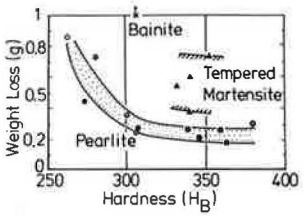

Figure 5. Relation between weight loss by wear test and superficial hardness after testing.

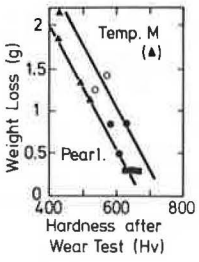

Figure 6. Rolling-contact fatigue-test method.

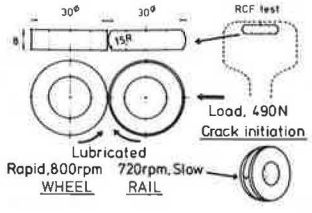

Figure 7. Relation between service life until surface-crack initiation by rolling-contact fatigue testing and rail-steel properties.

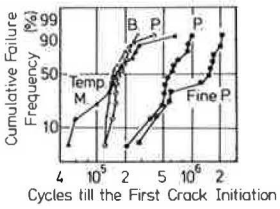

Figure 8. Preparation of fatigue-crack propagation test specimen.

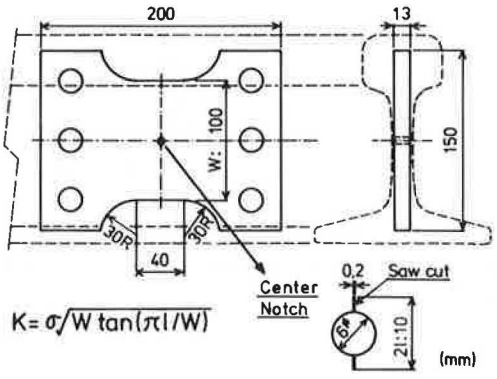

Table 1. Pearlitic-steel samples for fatigue-crack propagation (heat treatment and mechanical properties).

Sample Steel	Symbol	Heat Treatment[a]	GSN[b]	PS[c] (MPa)	TS (MPa)	El (%)	RA (%)	VHN
Carbon	A	1100°C AC	4.3	526	920	15	24	261
	B	900°C AC	5.9	476	875	18	26	243
1% Cr	C	900°C to 550°C IT	7.4	946	1279	15	40	382
	D	900°C to 650°C IT	7.4	777	1153	19	44	346
	E	1100°C to 550°C IT	3.5	963	1258	7	8	398
	F	1100°C to 650°C IT	3.5	630	1038	12	23	308
	G	900°C Q to 550° C T	-	1032	1213	16	35	370

Note: AC = air cooled; IT = isothermally transformed in salt bath; and Q, T = quenched and tempered.
[a] Austenitizing temperature. [b] American Society of Testing and Materials (ASTM) austenite. [c] 0.2 percent.

Table 2. As-rolled rails for fatigue-crack propagation rate and fracture toughness measurements: chemical composition.

Rail Steel	C	Si	Mn	P	S	Cr	Mo	Others
C[a]	0.78	0.23	0.97	0.018	0.025	-		
MC	0.54	0.37	1.43	0.021	0.006	1.01		0.05V
HS	0.72	0.92	1.37	0.022	0.010	-		
CV	0.74	0.29	1.30	0.021	0.011	0.79		0.12V
CVC	0.77	0.30	1.34	0.018	0.004	0.83		0.14V
CRM	0.76	0.15	0.86	0.014	0.006	0.69	0.18	
LC[b]	0.38	0.33	1.20	0.018	0.008	1.17	0.20	0.07V, B

[a]Standard carbon-steel rail. [b]Low-carbon bainitic-steel rail.

Table 3. As-rolled rails for fatigue-crack propagation rate and fracture toughness measurements: mechanical properties.

Rail Steel	Rail Size	PS (MPa)	TS (MPa)	El (%)	RA (%)	VHN	σwb[a] (MPa)
C	JRS60	502	902	16	31	302	365
MC	JRS60	624	1013	19	36	296	484
HS	JRS60	565	1010	16	22	288	424
CV	JRS60	699	1110	18	33	327	503
CVC	136RE	750	1200	11	26	358	582
CRM	136RE	686	1125	10	30	365	523
LC	JRS60	812	1080	17	31	324	493

[a]Rotating bending fatigue strength.

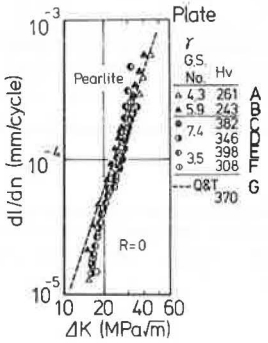

Figure 9. Fatigue-crack propagation rates of pearlitic steels.

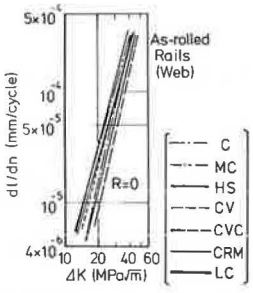

Figure 10. Fatigue-crack propagation rates of as-rolled rails.

pered martensite. The results are shown in Figure 9. Thus, Equation 1 holds true:

$$dl/dn = C(\Delta K)^m \quad (1)$$

where

$$\Delta K = \Delta\sigma\sqrt{W\tan(\pi l/W)} \quad (2)$$

where

l = half the length of crack,
W = specimen width, and
σ = gross weight.

The stress ratio is kept at zero. The crack propagation rate of each sample plate is nearly equal and is hardly affected by austenite grain size and strength. The broken line in Figure 9 shows the results for sample G, whose propagation rate is nearly the same as that of pearlitic steel.

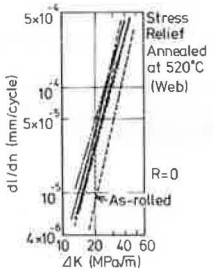

Figure 11. Fatigue-crack propagation rates of annealed specimens of as-rolled rails.

Next, the propagation rate was measured on the specimen cut from the web of as-rolled alloy-steel rail. The details of this specimen are shown in Tables 2 and 3. The results are shown in Figure 10. The same equation holds true on every rail but the propagation rates are slightly different, especially in the region of small ΔK and, as a whole, slower than those of Figure 9.

In Figure 11, the propagation rates measured on the annealed specimens of the as-rolled rail are shown. These specimens were annealed at 520°C for 30 min for stress relief. The propagation rate of the annealed specimen is higher than that of the as-rolled one, especially in the range of small ΔK.

Figure 12 illustrates an example of the longitudinal residual-stress pattern of an as-rolled rail specimen and an annealed specimen. The annealed specimen has been nearly relieved of all residual stress but, as in the as-rolled specimen, a fairly large amount of stress remains and, in particular, compressive stress exists in the vicinity of crack tips. This means that the difference in crack-propagation rates between as-rolled and annealed specimens is closely correlated to the residual stress, and the compressive residual stress retards crack propagation. With the growth of cracks, residual stress is gradually relieved, although compressive stress still remains at the tips of the crack. Therefore, the effect of residual stress becomes small in the region of a large ΔK. This effect can be well-understood if it is assumed that residual stress changes the stress ratio.

The fatigue fracture toughness, K_{IfC}, at room temperature and the fracture toughness, K_{IC}, at

0°C, and the material constants of fatigue of the samples in Tables 1-3 are listed in Table 4.

The K_{IfC} at room temperature for pearlitic steel is as follows (the number for G is for ductile fracture of tempered martensitic steel):

Symbol	K_{IfC}, as Received (MPa $\sqrt{m}$)
A	53.7
B	61.5
C	36.2
D	40.6
E	30.9
F	38.6
G	>92.9

K_{IfC} and K_{IC} are plotted against tensile strength in Figure 13. K_{IfC} decreases with an increase in tensile strength and, at the same strength level, the finer the austenite grain size, the higher the K_{IfC}. K_{IC} shows the same tendency as that of K_{IfC}, and each sample has K_{IC} nearly equal to K_{IfC}. The reason why K_{IfC} is hardly changed by annealing at 520°C is that, if the crack grows enough, the residual stress is almost completely relieved and has little effect on the as-rolled specimen. It is as if the stress in the as-rolled rail specimen had been relieved.

PRODUCTION OF HEAD-HARDENED RAIL AS HIGH-SERVICEABILITY RAIL

In the preceding section, increasing strength through pearlite refining, the reduction of nonmetallic inclusions, compressive residual stress, and austenite grain refinement were described as requisites for high serviceability. One type of rail that satisfies these requisites is the head-hardened rail. In this section, the production procedure of a head-hardened rail is reviewed. The chemical composition of this rail is the same as that of American Railway Engineering Association (AREA) standard rails and is as follows: C = 0.70-0.82 percent; Si = 0.10-0.25 percent; Mn = 0.70-1.00 percent; P = 0.040 percent, maximum and; S = 0.050 percent, maximum. After steelmaking by the Linz and Donawetz basic oxygen process (LD process), the steel is rolled into the shape of a rail by the same procedure as that for standard carbon-steel rails, which is as follows:

1. Steelmaking by the LD process,
2. Vacuum degassing and full killing,
3. Ingot making with hot top,
4. Blooming followed by slow cooling,
5. Bloom surface conditioning,
6. Reheating of blooms and rail rolling by universal mill,
7. Air cooling of the rail on cooling bed,
8. Roller straightening, and
9. Inspection and end conditioning.

Through these procedures, a clean and homogeneous ingot is secured and the shape of the rail is kept accurate. Recently, the production of the blooms by continuous casting has been increasing. The roller-straightened and inspected rail is transferred to the heat treatment works and head-hardened.

First the rail head is austenitized to a depth of about 25 mm from the running surface and on both sides by induction heating. Then this part is quenched by blown air so that the pearlite transformation proceeds nearly isothermally at 570-600°C in the circumferential zone at least 10 mm deep from the surfaces. It is noticeable that the temperature neither drops below 570°C nor rises above 600°C during pearlite transformation. This leads to the formation of an extremely fine pearlite and a specified hardness distribution. After heat treatment, bending or distortion hardly remains.

PROPERTIES OF HEAD-HARDENED RAIL

The objective properties of the hardened zone are as follows: tensile strength = 1180 MPa (120 kgf/mm²), minimum; elongation = 14 percent, minimum (gauge length = 3.54 x diameter); hardness of running surface = H_B 341-388; and hardness of transverse section = Hv 410, maximum.

The macrostructure of a transverse section of the rail head and the fine pearlitic microstructure of the hardened zone are shown in Figure 14. The depth of the hardened zone exceeds 18 mm. The interlamellar spacing of pearlite is about 0.13 μm. The austenite grain size is refined by about 2.5 American Society of Testing and Materials (ASTM) grain size numbers and, furthermore, the pearlite block

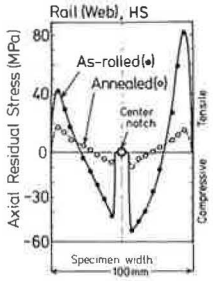

Figure 12. Longitudinal residual stress distribution of as-rolled or annealed crack propagation specimen (steel HS in Tables 2 and 3).

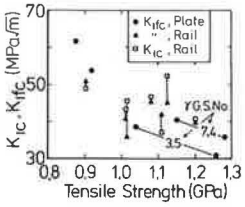

Figure 13. Relation between fracture toughness and tensile strength.

Table 4. Fracture toughness and material constants for fatigue-crack propagation.

Rail Steel	K_{IfC} at Room Temperature: As Received (MPa $\sqrt{m}$)	K_{IfC} at Room Temperature: Annealed (MPa $\sqrt{m}$)	K_{IC} at 0°C, As Received (MPa $\sqrt{m}$)	Constants, m and C[a]: As Received, m	As Received, C	Annealed, m	Annealed, C
C	51.0	52.3	49.0	3.43	9.62×10^{-10}	4.10	5.84×10^{-11}
MC	35.8	35.8	45.7	3.27	2.49×10^{-9}	3.32	1.31×10^{-9}
HS	40.9	40.9	43.5	3.68	5.67×10^{-10}	3.84	1.19×10^{-10}
CV	42.0	38.1	37.2	3.83	3.87×10^{-10}	3.62	3.72×10^{-10}
CVC	40.1	38.5	40.6	4.09	1.47×10^{-10}	4.14	2.94×10^{-11}
CRM	45.1	45.4	52.3	3.22	1.91×10^{-9}	3.23	1.30×10^{-9}
LC	45.4	45.4	46.7	3.43	9.62×10^{-10}	3.43	9.62×10^{-10}

[a]Constants for fatigue-crack propagation rate equation $dl/dn = C(\Delta K)^m$ · (mm/cycle).

Table 5. Example of mechanical properties of head-hardened carbon-steel rail.

Specimen Condition	PS (MPa)	TS (MPa)	El (%)	RA (%)	H_B	σwb (MPa)	K_{IC}[a] (MPa $\sqrt{m}$)	WL[b] (g)
Hardened zone	849	1250	16	37	363	559	48	0.19
As rolled	575	958	14	20	-	343	43	-

[a]Fracture toughness at −20° C. [b]Weight loss by wear test.

Figure 14. Macrostructure of transverse section of head and microstructure of hardened zone of head-hardened carbon-steel rail.

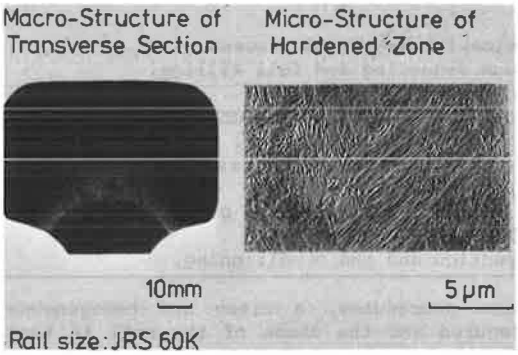

Figure 15. Example of hardness change in transverse section of head-hardened carbon-steel rail.

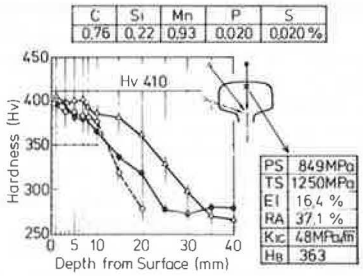

Figure 16. Longitudinal residual stress on surface of as-rolled or head-hardened rails.

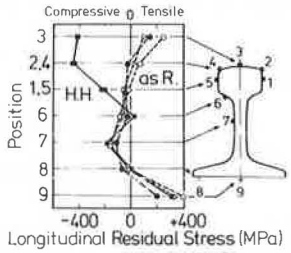

Figure 17. Bending fatigue strength of as-rolled or head-hardened rails in comparison with tensile strength.

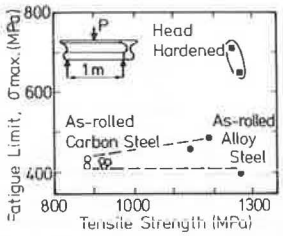

Figure 18. Comparison of wear depth of head-hardened rails with that of as-rolled carbon-steel rails.

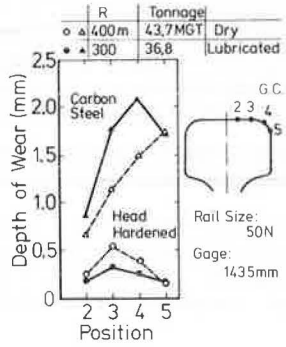

Figure 19. Wear depth of gauge side surface of head-hardened carbon-steel rails.

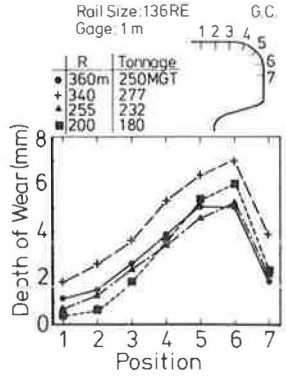

size is also refined through heat treatment. The hardness change in a transverse section is shown in Figure 15. The hardness is highest at the surface and then decreases gradually and smoothly inward. A hardness of Hv 350 is obtained at the point 10 mm from the surface. The mechanical properties of the hardened zone are shown in Table 5 with those before hardening. The chemical composition of the head-hardened carbon-steel rail is as follows: C = 0.77 percent, Si = 0.22 percent, Mn = 0.95 percent, P = 0.019 percent, and S = 0.021 percent. Fracture toughness is fairly high in spite of high strength. Weight loss from the Nishihara-type wear test is about 0.2 g, which coincides well with the expected value.

The longitudinal residual stress on the rail surface was measured on as-rolled carbon-steel rail and head-hardened rail. The results are shown in Figure 16 with those of the as-rolled alloy-steel rails. The as-rolled rails possess tensile residual stress at the rail head and center of the base. Compressive stress exists in the web, which caused the retardation of fatigue-crack propagation, as shown in Figure 10. The tensile residual stress on the rail head turns into a compressive stress of about 400 MPa through head-hardening, but the stress remains unchanged at the web and base that are not heat treated.

In order to check how the residual stress on the rail surface affects fatigue strength, actual rails were fatigue tested by three-point bending with the rail head subjected to tensile stress (6). The bending fatigue strength is plotted against the tensile strength of the rail head in Figure 17. Al-

though some problems remain in this fatigue-test method in view of actual track conditions, the head-hardened rails exhibit fairly higher fatigue-strength values than those of the as-rolled rails of the nearly same tensile strength. This difference is caused not only by residual stress but also by surface conditions, e.g., surface roughness. The rotating bending fatigue strength measured on cut-out specimens that are free from residual stress and surface conditions is proportional to their tensile strength and can be expressed by the following equation, as with other steels:

$$\sigma w = 0.646 \times (\text{tensile strength}) - 227(\text{MPa}) \quad (3)$$

Therefore, the importance of residual stress in fatigue strength should always be taken into consideration.

As stated above, this head-hardened rail satisfies most of the requisites for high serviceability. The wear behavior of this rail in actual tracks is as follows. Figure 18 shows the wear on the gauge side of high rail under an axle load of 22-25 tons and traffic tonnage of about 40 million gross tons (MGT). The maximum wear of the gauge corner is less than one-third of that of standard carbon-steel rail. Figure 19 also shows the wear on the gauge side of high rail under an axle load of 25 tons and traffic tonnage of about 200 MGT. The maximum wear of the gauge corner is about 5-7 mm and surface defects are hardly observed except for some flakings on the running surface. Low side rail exhibits little metal flow.

At the beginning of production, it was not necessarily intended that this rail satisfy the above-mentioned requisites, but this rail seems to possess high serviceability for heavy-load railways and has exhibited good performance in many railways. Remaining problems, if they exist, will be in welding and corrugation.

CONCLUSION

As the result of investigations into the requisites for rails of high serviceability, increasing the strength of rails through the refining of pearlite, compressive residual stress, and austenite grain refinement has proved to be effective in prolonging the service life of rails. One type of rail that satisfies these requisites is the head-hardened rail, which possesses a tensile strength that exceeds 1200 MPa, a very fine pearlitic microstructure, and a compressive residual stress of about 400 MPa in the hardened zone. This rail has exhibited good performance with less wear, fewer defects, and less metal flow in many heavy-load railways.

REFERENCES

1. H. Masumoto, K. Sugino, and H. Hayashida. Development of Wear Resistant and Anti-Shelling High-Strength Rails in Japan. Presented at Heavy Haul Railways Conference, Perth, Australia, 1978.
2. H. Masumoto, K. Sugino, S. Nishida, R. Kurihara, and S. Matsuyama. Some Features and Metallurgical Considerations of Surface Defects in Rail Due to Contact Fatigue. In Rail Steels--Developments, Processing, and Use, ASTM Special Tech. Publ. 644, Philadelphia, 1978, pp. 233-255.
3. D.E. Sonon, J.V. Pellegrino, and J.M. Wandrisco. Metallurgical Examination of Control-Cooled, Carbon-Steel Rails with Service-Developed Defects. In Rail Steels--Developments, Processing, and Use, ASTM Special Tech. Publ. 644, Philadelphia, 1978, pp. 99-117.
4. S. Marich, J.W. Cottam, and P. Curcio. Laboratory Investigation of Transverse Defects in Rails. Presented at Heavy Haul Railways Conference, Perth, Australia, 1978.
5. S. Nishida, T. Urashima, K. Sugino, and H. Masumoto. Study on Fatigue Crack Propagation of Rail Steels. Proc., International Conference on Strength of Metals and Alloys, 1979, pp. 1255-1260.
6. C. Urashima, S. Nishida, K. Sugino, and H. Masumoto. Fatigue Strength of the Rail. Trans., I.S.I.J., Vol. 21, 1981, p. B-40.

Publication of this paper sponsored by Committee on Track Structure System Design.

Rail Manufacture in Great Britain

JOHN D. YOUNG

A review of the history of rail manufacture in Britain, together with current and future plant and process routes, is presented. British capability to meet current and predicted future rail requirements is associated with modern steelmaking process routes, specialized rail manufacturing plants, long experience in supplying the varied needs of railroads internationally, and a market-oriented management philosophy. Current American dimension requirements present no problems, as routine manufacture meets stricter British and European standards. The continuous casting of rail steel and the prohibition of aluminum deoxidation are claimed as major factors that limit the size and number of complex alumino-silicate inclusions in the production of clean rail steels. Other process-route parameters also contribute. Future rail requirements of a metallurgical nature (e.g., clean, low-hydrogen steel) and of a geometric type (e.g., better section and straightness control) are discussed. The urgent need for better track and vehicle maintenance standards is strongly emphasized. The large American rail market and the considerable standardization of rails could be expected to encourage specialization and development of advanced rail-making technology. Low home-market rail prices and limited involvement in more sophisticated international rail markets may have inhibited such developments.

The evolution of, and advances made in, rail technology have resulted in more stringent requirements being incorporated in many rail specifications. Metallurgical, mechanical, and geometric aspects are now of greater importance than in the past due to more severe rail track and traffic conditions, e.g., the use of higher axle loads, increased traffic speeds, the adoption of diesel or electric traction, and the use of continuously welded track.

The ability of the rail manufacturer to meet the more stringent requirements is affected, to varying degrees, by a number of factors, which include the following:

1. The processes used and plant available for steelmaking, casting, rolling, and finishing of the rails;